DNA Recognition by the Helix–Turn–Helix Motif: Investigation by Laser Raman Spectroscopy of the Phage λ Repressor and Its Interaction with Operator Sites O_L1 and O_R3†

James M. Benevides,‡ Michael A. Weiss,§,‖ and George J. Thomas, Jr.*,‡

Division of Cell Biology and Biophysics, School of Basic Life Sciences, University of Missouri—Kansas City, Kansas City, Missouri 64110, and Department of Biological Chemistry and Molecular Pharmacology, Harvard Medical School, Boston, Massachusetts 02115

Received October 16, 1990; Revised Manuscript Received February 19, 1991

ABSTRACT: The λ repressor provides a model system for biophysical studies of DNA recognition by the helix–turn–helix motif. We describe laser Raman studies of the λ operator sites O_L1 and O_R3 and their interaction with the DNA-binding domain of λ repressor (residues 1–102). Raman spectra of the two DNA sites exhibit significant differences attributable to interstrand purine–purine steps that differ in the two oligonucleotides. Remarkably, the conformation of each operator is significantly and specifically altered by repressor binding. Protein recognition, which involves hydrogen-bond formation and hydrophobic contacts in the major groove, induces subtle changes in DNA Raman bands of interacting groups. These include (i) site-specific perturbations to backbone phosphodiester geometry at AT-rich domains, (ii) hydrophobic interaction at thymine $5CH_3$ groups, (iii) hydrogen bonding to guanine 7N and 6C=O acceptors, and (iv) alterations in sugar pucker within the C2′-endo (B-DNA) family. These perturbations differ between aqueous O_L1 and O_R3 complexes of repressor, indicating that protein binding in solution determines the precise DNA conformation. The overall structure of the λ domain is not greatly perturbed by binding to either O_L1 or O_R3, in accord with X-ray studies of other complexes. However, Raman markers indicate a change in hydrogen bonding of the OH group of tyrosine-22, which is a hydrogen-bond acceptor in the absence of DNA but a combined donor and acceptor in the O_L1 complex; yet, Y22 hydrogen bonding is not altered in forming the O_R3 complex. The present results demonstrate qualitatively different and distinguishable modes of interaction of the λ repressor DNA-binding domain with operators O_L1 and O_R3 in solution. This application of laser Raman spectroscopy to a well-characterized system provides a prototype for future Raman studies of other DNA-binding motifs under physiological conditions.

Protein–DNA recognition is accomplished by families of related structural motifs, such as the helix–turn–helix (HTH), leucine zipper (bZIP), and zinc finger, which constitute discrete DNA-binding domains. The most thoroughly studied of these is the HTH motif. X-ray diffraction of phage repressor–operator co-crystals provides a high-resolution view of representative HTH-DNA complexes. Such studies have revealed unifying features of the mechanism of HTH recognition and have demonstrated the importance of detailed stereochemical interactions in lieu of a simple "recognition code". A striking example is provided by co-crystals of phage 434 operator with HTH repressors, 434 Cro and 434 cI. The operator adopts a different conformation in each complex, demonstrating that protein binding influences the orientation of functional groups in the major groove (Wolberger et al., 1988). This conclusion, deduced from the crystal structures, may also apply to repressor–operator complexes in solution, although direct evidence from comparison of solution structures has not yet been obtained. Since small differences in affinity between operator sites can be sufficient to define a genetic switch (Ptashne, 1987), these effects may be of central biological importance.

In the present work we demonstrate that binding of the λ repressor HTH influences differently the conformations of two λ operator sites, O_L1 and O_R3. The operator sequences (Figure 1) differ only at base-pairs 3′, 5′, and 8′ of their nonconsensus half-sites; yet, repressor affinities for O_L1 and O_R3 differ 50-fold, an essential feature of the phage regulatory pathway. Biochemical footprinting indicates that λ repressor recognizes both operator sites similarly. The structural basis for site discrimination, as inferred from studies of the O_L1 co-crystal (Jordan & Pabo, 1988) and from properties of genetically altered repressors (Eliason et al., 1985), may be due to recognition of GC at base-pair 8 by the N-terminal arm. λ repressor does not distinguish between TA and CG at base-pair 3, but the thymine methyl group of base-pair 5 makes important hydrophobic contacts with repressor side chains. Structures of O_L1 and O_R3 in the absence of repressor and of the O_R3 complex have not been determined.

The present investigation seeks to address the following questions: Do the solution conformations of related operator sites differ? How may such differences relate to repressor recognition and binding? Is the solution structure of a representative HTH domain influenced by operator binding? Are the salient structural features of repressor–operator co-crystals maintained in solution? Because of previous extensive characterizations, the λ repressor system provides an appropriate model in which to explore these questions. Our results are presented in three parts. In part I the effects of specific DNA

† Paper XLII in the series Raman Spectral Studies of Nucleic Acids, supported by grants from the National Institutes of Health to G.J.T. (AI18758) and M.A.W. (HD26465).

* To whom correspondence should be addressed.
‡ University of Missouri—Kansas City.
§ Harvard Medical School.

‖ M.A.W. is supported in part by the Pfizer Scholars Program for New Faculty and an American Cancer Society Junior Faculty Research Award.

0006-2960/91/0430-5955$02.50/0

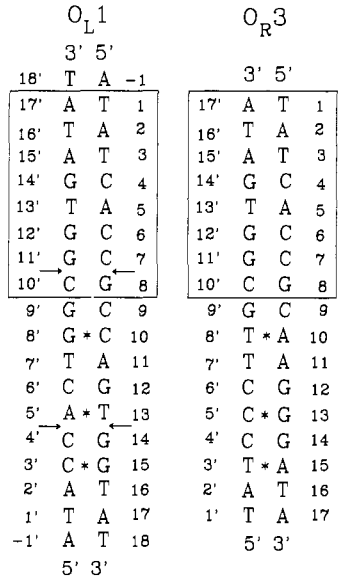

FIGURE 1: Schematic diagram of the base sequences of O_L1 and O_R3. The consensus sequence of each operator is enclosed by a box. The base-pairs that differ between operators in the nonconsensus half-sites are distinguished by asterisks. The arrows in the O_L1 sequence point to the steps where backbone torsions α, β, and γ may assume the all-trans (t/t/t) configuration, as discussed in the text.

binding on the structure of the λ domain are investigated. It is shown that only local adjustments of side chains are required for ligand recognition. In part II the solution conformations of O_L1 and O_R3 are shown to exhibit distinguishable B-family secondary structures. In part III the effects of protein binding on operator conformation are examined. We show that the conformation of each operator is significantly and specifically altered by repressor binding. In a related paper (Benevides et al., 1991b) we have examined nonlocal effects of repressor quaternary structure in recognition and binding of specific operator sites. These studies should provide a foundation for the more general application of laser Raman spectroscopy to problems in protein–nucleic acid recognition, including study of complexes of bZIP and Zn-finger proteins.

Materials and Methods

(I) Preparation and Purification of λ Repressor

The N-terminal fragment of wild-type λ repressor (residues 1–102), here abbreviated RF, was overexpressed in *Escherichia coli* and purified as described (Sauer et al., 1986). The purified proteins were exhaustively dialyzed against 0.2 M NH_4HCO_3 and lyophilized. Lyophilizates were redissolved in 0.2 M NaCl. The protein was >98% pure as determined by sodium dodecyl sulfate–polyacrylamide gel electrophoresis (SDS–PAGE). The operator-binding domain is a dimer at the concentrations employed for Raman spectroscopy (Sauer et al., 1986; Weiss et al., 1987).

(II) Synthesis and Purification of Operator DNA Sites

O_L1 (molecular mass 12336 Da) was synthesized as asymmetric 19-base oligonucleotides by the DNA Synthesis Service, Department of Chemistry, University of Pennsylvania, Philadelphia, PA 19104. Its sequence is shown in Figure 1. The strands were combined in equimolar proportions (as determined from UV absorbance measurements at 260 nm) and annealed by heating to 50 °C, followed by slow cooling. The solution of the duplex was lyophilized to near dryness and redissolved at concentrations of 25 and 50 mg/mL in 0.2 M NaCl. In each case, the pH was adjusted to 7.8 ± 0.2 by the addition of dilute NaOH. The percent base composition is A = T = 52.6% and G = C = 47.4%.

O_R3 (molecular mass 10963 Da) was synthesized as asymmetric 17-base oligonucleotides by Pharmacia, Ltd. (Japan) and annealed as described above. The duplex was separated from excess single strands on a Sephadex G75 column. Following desalting on a Sephadex G10 column, pyridine cation was converted to sodium cation on a DEWAX ion-exchange column. Paramagnetic metal impurity was then eliminated by passing the duplex over a Chelex column. The duplex was lyophilized to near dryness and redissolved at a concentration of 25 mg/mL in 0.2 M NaCl, and the pH was adjusted to 7.5 ± 0.2 with dilute NaOH. The percent base composition is A = T = 52.9% and G = C = 47.1%.

(III) Preparation of Repressor–Operator Complexes

Repressor–operator complexes were prepared by dissolving the appropriate weight of operator (O_L1 or O_R3) in a solution containing 50 mg/mL repressor. Complexes containing 1:1 and 2:1 molar ratios of repressor monomer to operator duplex were investigated for O_L1. The 1:1 ratio provides a solution in which virtually all repressor is bound to DNA but contains an approximate 50% molar excess of protein-free DNA. The 2:1 ratio at equilibrium contains predominantly (>80%) complexed material. For O_R3, only the 2:1 complex was studied.

(IV) Raman Spectroscopy

Solutions were sealed in glass capillary cells (Kimax No. 34507) that were thermostated at 12 °C in the sample illuminator of the spectrometer while Raman spectra were recorded. For operators, repressors, and their complexes, spectra were obtained over the interval 300–1800 cm^{-1}. All spectra were excited with the 514.5-nm line of a Coherent Innova 70 argon laser and were recorded on a Spex Ramalog V/VI spectrometer under the control of an IBM-XT microcomputer. Data were collected at increments of 1 cm^{-1} with an integration time of 1.5 s and spectral slit width of 8 cm^{-1}. Each Raman spectrum of the 300–1800-cm^{-1} interval displayed in the illustrations is the unsmoothed average of eight to ten scans, of 1.5 cm^{-1} or better repeatability. Additional signal averaging was employed for scans over narrower spectral intervals, such as the Raman amide I and amide III intervals. In all cases, the scattering by the aqueous solvent was compensated by use of computer subtraction techniques described previously (Benevides et al., 1984). The Raman frequencies reported for discrete peaks in the spectra are accurate to within ±1.5 cm^{-1}.

In the computation of DNA difference spectra, the band at 1092 cm^{-1} serves as a reliable intensity standard. This band, assigned to the symmetric P–O stretching vibration of the PO_2^- group (Thomas, 1970), is nearly constant in intensity for B-DNA over a wide range of ionic strengths and temperatures (Prescott et al., 1984). In the case of viruses and other nucleoprotein complexes, the 1092-cm^{-1} band is partially overlapped by somewhat weaker bands due to protein but still serves satisfactorily as an internal intensity standard (Thomas, 1987). We expect this to be true also for Raman spectra of repressor–operator complexes.

For each protein, nucleic acid, and complex, Raman spectra were collected in duplicate on independently prepared samples. As many as five separate runs were made for the proteins, four for DNA operators. Spectra obtained from separate runs on a given sample were indistinguishable within the noise level of the spectra; i.e., intensities did not differ by more than 4% for the marker bands used in structural interpretations. We have employed the following criteria for selection and dis-

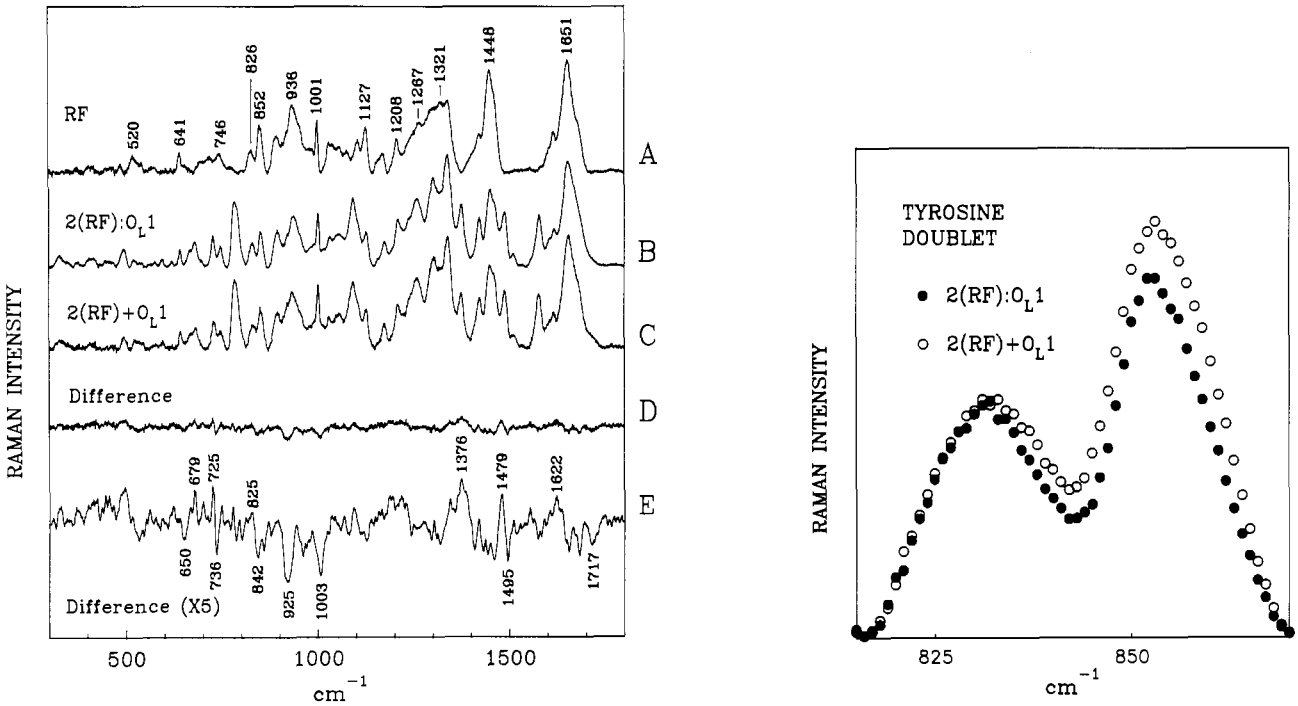

FIGURE 2: (Left panel) Raman spectra in the 300–1800-cm^{-1} region of (A) the N-terminal fragment of λ repressor (residues 1–102), (B) the 2:1 complex of repressor and O_L1, (C) the sum of the spectral constituents (repressor and O_L1), (D) the computed difference of the complex minus the sum of the constituents (B − C), and (E) a 5-fold amplification of the difference spectrum (D) after 11-point smoothing. (Right panel) Expanded Raman spectra in the region 815–870 cm^{-1} showing different profiles of the complex [2(RF):O_L1, ●] and the sum of the constituents [2(RF) + O_L1, ○]. The DNA contribution is less than 10% of the 826-cm^{-1} intensity in each spectrum and is assumed constant. The difference is attributable to altered hydrogen bonding of repressor tyrosine. [See text and Thomas et al. (1986a).] Data points were obtained from each sample by signal averaging (20 scans, 4-s integration time/point); identical results were obtained in duplicate protocols. Data point reproducibility and estimated limit of error are within the size of the circle. Relative intensities are normalized to the 826-cm^{-1} band.

cussion of significant difference features. First, a difference band is deemed to have significant intensity if it reflects *both* a relative intensity change of at least 10% in comparison to its parent bands *and* a signal-to-noise ratio of at least 2:1 in the difference spectrum computed from multiply averaged minuend and subtrahend spectra. Second, the difference band must be structurally interpretable. Thus, while a difference band may in principle be significant by the first criterion, it may be impossible to interpret in sufficient detail to warrant discussion. However, there are few bands in the present spectra that meet only the first criterion.

Results and Interpretation

(I) Raman Spectra of the HTH Domain and Effects of Operator Binding

(A) Secondary Structure. The spectrum of the 1–102 repressor HTH fragment (RF) is shown as spectrum A in Figure 2. The amide bands indicate a predominance of α-helix (Thomas et al., 1986a), in agreement with the 1–92 crystal structure (Pabo & Lewis, 1982). Spectrum D in Figure 2 is the difference between the spectrum of the 2:1 complex [2(RF):O_L1, spectrum B] and the sum of constituents [2(RF) + O_L1, spectrum C]. It shows the absence of major secondary structure changes of RF with formation of the O_L1 solution complex; the small changes reflect structural adjustments in side chains and DNA. Figure 3 shows corresponding data for the 2:1 complex of RF with O_R3 [2(RF):O_R3]. No major secondary structure change is apparent; but again small difference bands reflect minor structural adjustments in the O_R3 complex. Importantly, the difference spectra of Figures 2 and 3 are inequivalent, which clearly indicates that constituents of 2(RF):O_L1 and 2(RF):O_R3 undergo *different* structural adjustments with complex formation. The nature of these

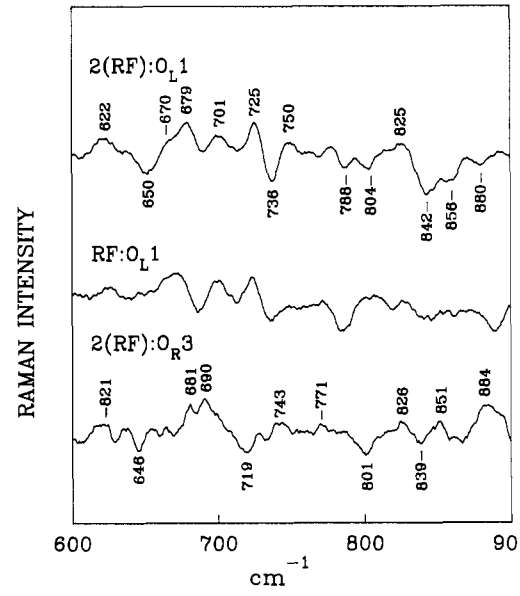

FIGURE 3: Raman spectra in the 300–1800-cm^{-1} region of (A) the 2:1 complex of repressor and O_R3, (B) the sum of the spectral constituents (repressor and O_R3), (C) the computed difference of the complex minus the sum of the constituents (A − B), and (D) a 5-fold amplification of the difference spectrum (C) after 11-point smoothing.

conformational differences is next discussed.

(B) Tyrosine Environments. In the right panel of Figure 2, we compare the important tyrosine doublet region for the 2(RF):O_L1 complex and sum of constituents to illustrate the significance of minor intensity changes referred to above. Figures 4 and 5 show other significant, but minor, intensity changes with complex formation. The tyrosine doublet ratio, I_{852}/I_{826}, reflects the distribution of phenolic OH groups among hydrogen-bond acceptor (A), donor (D), and simultaneous

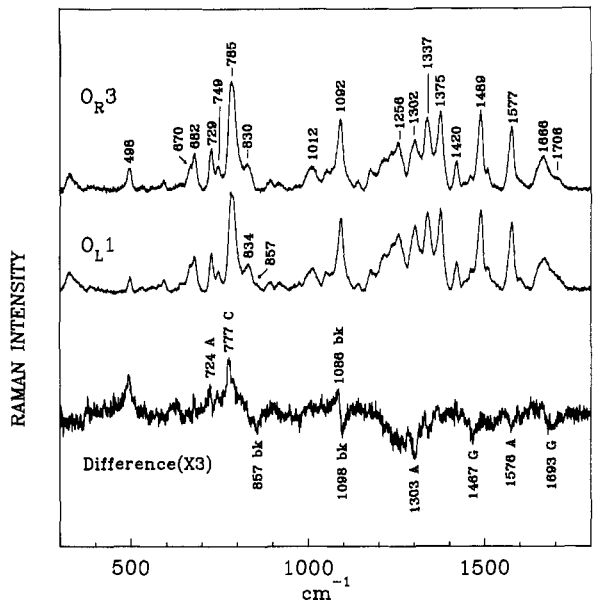

FIGURE 4: Difference spectra in the region 600–900 cm^{-1} for the following repressor–operator complexes: 2(RF):O_L1 (2:1 complex), top; RF:O_L1 (1:1 complex), middle; and 2(RF):O_R3 (2:1 complex), bottom. In each case, the difference spectrum was computed as the complex minus the sum of the constituents with use of the data of Figures 2 and 3.

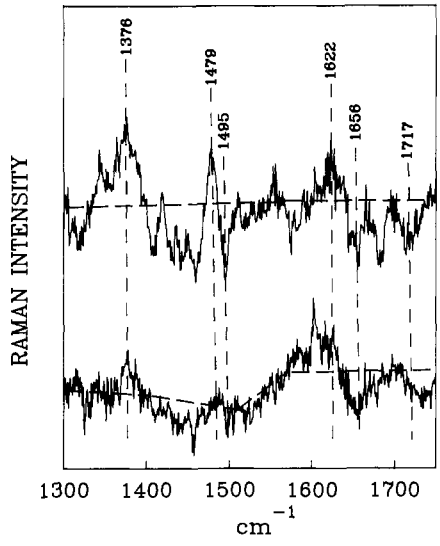

FIGURE 5: Difference spectra in the region 1300–1700 cm^{-1} for the following repressor–operator complexes: 2(RF):O_L1 (2:1 complex), top; and 2(RF):O_R3 (2:1 complex), bottom. Other conditions are as in Figure 4.

acceptor/donor (E) states (Siamwiza et al., 1975). In the absence of DNA (spectrum A, Figure 2) this ratio is 2.05, indicating 3A + 2E tyrosines. These states have been assigned to individual residues by a combination of chemical modification and site-specific mutagenesis as follows: Y22 (A), Y60 (E), Y85 (A), Y88 (A), and Y101 (E) (Thomas et al., 1986a). Although the determination of I_{852}/I_{826} is complicated by overlapping DNA bands, the doublet is well resolved and accurately measurable (Figure 2, right panel, and Figure 4). Thus, I_{852}/I_{826} decreases to 1.75 ± 0.05 in 2(RF):O_L1. The sign and magnitude of the intensity change indicates the transfer of one tyrosine from an exclusive hydrogen-bond acceptor (A state) to both a hydrogen-bond donor and acceptor (E state). More complicated schemes cannot be excluded but would appear to be less likely given the absence of overall conformational change in the protein backbone.

Table I

Backbone Conformation Markers[a]			
group	A-DNA	Z-DNA	B-DNA
OPO	706 ± 5		790 ± 3
	807 ± 3	745 ± 3	828 ± 2 (GC)
			835 ± 2 (GC/AT)
			839 ± 2 (AT)
PO_2^-	1099 ± 1	1095 ± 1	1092 ± 1
CH_2	1418 ± 2	1425 ± 2	1422 ± 2

Nucleoside Conformation Markers[a]			
base	C3-endo/anti	C3-endo/syn	C2-endo/anti
G	664 ± 2	625 ± 3	682 ± 2
A	1335 ± 2	1310 ± 5	1339 ± 2
C	1252 ± 2	1265 ± 2	1255 ± 5
T	662 ± 2	650 ± 2	669 ± 2
	745 ± 2	770 ± 2	748 ± 2

[a] Frequencies of marker bands (cm^{-1}) were determined from Raman spectra of crystals and fibers of known structures (Thomas & Wang, 1988; Dijkstra et al., 1991).

A contrasting feature between difference spectra of 2(RF):O_L1 and 2(RF):O_R3 (Figure 4) is that a significant change in I_{852}/I_{826} occurs only for the former. The invariance of tyrosine hydrogen bonding in the 2(RF):O_R3 complex is consistent with locally different modes of RF interaction with O_L1 and O_R3. This result suggests that tyrosine interactions monitored by Raman spectroscopy may be generally useful for discriminating repressor binding between closely related operators.

(C) Other Side Chain Environments. For both 2(RF):O_L1 and 2(RF):O_R3, Raman difference intensities are assignable to C_α–C_β stretching of various aliphatic side chains (925 cm^{-1}) and to aromatic ring stretching of phenylalanine (1000 cm^{-1}). Although a more detailed structural interpretation of these intensity differences is presently not possible, it is clear that they are markedly different for RF interactions with O_L1 and O_R3. Crystal structures of the 1–92 fragment with and without DNA also indicate local conformational changes affecting side-chain residues within the hydrophobic core (Pabo & Lewis, 1982; Jordan & Pabo, 1988).

(II) Raman Spectra of λ Operators

Raman studies of mononucleotide and oligonucleotide single crystals, characterized structurally by X-ray diffraction, have permitted the establishment of a library of Raman bands or markers that are diagnostic of DNA conformation (Nishimura et al., 1986; Thomas & Wang, 1988). Two major categories of Raman marker bands have emerged from these studies. Bands in the first category, referred to as *backbone* conformation markers, are sensitive to changes in torsions of the P–O5′–C5′–C4′–C3′–O3′–P network but do not depend strongly upon the identity of the base attached at C1′. [The designated backbone torsion angles are α (P–O5′), β (O5′–C5′), γ (C5′–C4′), δ (C4′–C3′), ϵ (C3′–O3′), and ζ (O3′–P)]. Bands of the second category, termed *nucleoside* conformation markers, arise predominantly from ring–atom stretching vibrations of the DNA bases, which are strongly coupled mechanically through the glycosyl bond to C–C and C–O stretching vibrations of the attached furanose ring. For a given base, a nucleoside conformation marker is typically sensitive to furanose pucker (C4′–C3′ torsion angle δ) and glycosyl bond orientation (C1′–N torsion angle χ). Table I provides an abbreviated listing of Raman backbone and nucleoside conformation markers that serve as the foundation for analysis of λ operators presented below.

(A) B-DNA Secondary Structure. Raman spectra of O_L1 and O_R3 in the region 300–1800 cm^{-1} are shown in Figure 6.

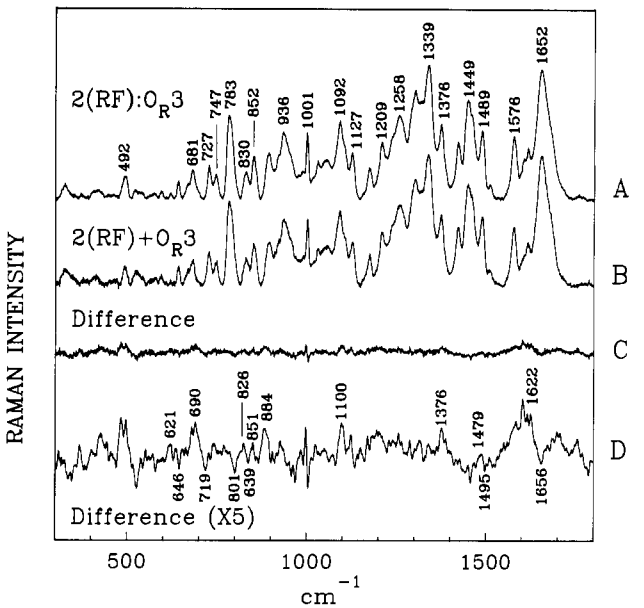

FIGURE 6: Raman spectra in the region 300–1800 cm^{-1} of O_R3, top; O_L1 middle, and the computed difference spectrum, $O_R3 - O_L1$, bottom. Experimental conditions and sequences are described in the text and Figure 1. In computation of the difference spectrum, the band near 1090 cm^{-1} was used as the basis for normalization of intensities.

Major bands in these spectra are assigned by analogy with the spectrum of the B-DNA dodecamer [d-(CGCAAATTTGCG)]$_2$ analyzed previously (Benevides et al., 1988). Raman bands sensitive to phosphodiester and nucleoside conformation are similar for both operator sites and are characteristic of right-handed B-DNA (Table I). In particular, both operators exhibit the characteristic C2′-endo/anti guanosine marker at 682 cm^{-1} as well as other nucleoside conformation markers indicative of C2′-endo/anti deoxyribose conformers exclusively.

(*B*) *Differences between Operator Sites.* Although the above similarities identify both O_L1 and O_R3 as members of the B-DNA family, the peaks and troughs in the difference spectrum of Figure 6 indicate structural differences. Since the overall base compositions are essentially the same (≈52% AT and ≈47% GC), these differences must originate from sequence-dependent variations in secondary structure and involve the nonconsensus half-sites (Figure 1). Differences are most pronounced in two spectral regions, 700–900 and 1200–1400 cm^{-1}. The first region contains bands most sensitive to phosphodiester conformation (800–880 cm^{-1}) and exhibits the following features. (i) The principal B-form backbone marker of O_L1 is diffuse and centered at 834 cm^{-1}, whereas that of O_R3 is peaked at 830 cm^{-1}. (ii) O_L1 has a weak band at 857 cm^{-1}, which is absent for O_R3. The 857-cm^{-1} band of O_L1 exhibits about one-tenth the intensity of the major 834-cm^{-1} band in the same spectrum. (iii) O_R3 exhibits no band at 857 cm^{-1} and about 10% greater intensity than O_L1 in the region 800–830 cm^{-1}. The observed differences between O_L1 and O_R3 cannot be attributed to differences in sugar pucker or glycosyl torsion, since we detect furanose conformers only of the C2′-endo/anti family (Table I). Accordingly, the spectral differences must originate in other torsions of the phosphodiester backbone.

(III) Changes of DNA Structure Attendant with Repressor Binding

(*A*) *Backbone and Nucleoside Conformation.* Figure 4 shows Raman difference spectra in the 600–900-cm^{-1} region for O_L1 and O_R3 complexes. In the case of the O_L1 complex, the most striking feature is the negative band near 842 cm^{-1}, assignable to the DNA backbone (Table I) and indicating altered OPO torsions at several AT pairs with repressor binding. On the basis of the difference-band intensity at 842 cm^{-1}, we estimate that at most 4 AT base-pairs/oligonucleotide complex are affected by RF binding. Also assigned to DNA are positive intensity differences at 622, 670, 679, 725, 750, and 825 cm^{-1} and negative differences at 650, 736, 788, 804, 856, and 880 cm^{-1}. Although complicated in origin, these bands are associated primarily with AT pairs (Thomas et al., 1986b) and indicate that dA and dT nucleoside conformations are more significantly altered than those of dG and dC by RF binding to O_L1. Our results are consistent with those of X-ray crystallography: AT-rich ends of the repressor-bound operator differ from canonical B-DNA more significantly than the central GC-rich domain (Jordan & Pabo, 1988).

For the 2(RF):O_R3 complex, the pattern of peaks and troughs in the difference spectrum differs considerably from that seen for the 2(RF):O_L1 complex. The deep negative intensity at 842 cm^{-1} characteristic of the O_L1 complex is replaced by a much smaller negative inflection, centered at 839 cm^{-1}. This band is still assignable to OPO torsions of AT pairs in the DNA backbone, but the smaller intensity difference indicates that fewer OPO torsions of AT base-pairs are affected when repressor forms the 2(RF):O_R3 complex. The position and intensity of Raman nucleoside marker bands in the difference spectrum of Figure 3 indicate that the nucleoside conformation, in general, is also less perturbed with the formation of the 2(RF):O_R3 complex. All nucleoside types appear to undergo small rearrangements in sugar pucker and glycosyl torsion.

(*B*) *Purine-Specific Interactions.* In addition to sugar and phosphate conformations, the Raman spectrum monitors hydrogen-bonding interactions of the guanine 7N acceptor. In guanine mononucleotides and in B-DNA, the guanine ring generates an intense band near 1490 cm^{-1} (Lord & Thomas, 1967; Small & Peticolas, 1971). This band shifts to about 1480 cm^{-1} when 7N accepts a strong hydrogen bond as in Hoogsteen complexes or is coordinated to divalent metal ions (Hartman et al., 1973; Nishimura et al., 1986). Figure 5 shows the O_L1- and O_R3-specific difference spectra in the 1300–1700-cm^{-1} region. For both O_L1 and O_R3, we observe a shift of Raman intensity from 1490 to 1480 cm^{-1} with complex formation, providing direct evidence of hydrogen-bond formation between repressor side chains and 7N sites. For the O_L1 complex, the magnitude of the intensity shift is consistent with a *minimum* of 2 dG residues hydrogen bonded at 7N. For O_R3 no significant frequency shift is apparent. [Because contributions from protein Raman bands partially overlap this spectral region of DNA, and because the resolution of the 1490- and 1480-cm^{-1} components is incomplete, the number of interacting guanine residues could be underestimated by our measurements. We note, for example, that four guanine 7N contacts are observed per operator in the crystal structure of the O_L1 complex (Jordan & Pabo, 1988).] Our results indicate that the number of guanine 7N contacts per O_R3 duplex is reduced compared with the O_L1 complex.

Also specific to the O_L1 complex, we observe a strong negative band at 1717 cm^{-1} in the difference spectrum of Figure 5. This band is assigned with confidence to a carbonyl group stretching frequency. Ordinarily, the frequency of a C=O stretching vibration increases with decreasing hydrogen-bonding strength (Bellamy, 1980; Prescott et al., 1984; Benevides et al., 1988). We presume that the elevated C=O

frequency in the sum-of-constituents spectrum (generating the trough at 1717 cm^{-1} in the difference spectrum) reflects carbonyls less strongly hydrogen bonded in the protein-free O_L1 operator than in the 2(RF):O_L1 complex. This band is believed to represent the effect of guanine 6C=O interactions with repressor residues in the 2(RF):O_L1 complex. Such interactions are observed in the co-crystal structure, involving 6C=O acceptors of G14′ and G12′ with, respectively, O-H and N-H donors of S45 and K4 (Jordan & Pabo, 1988). The 2(RF):O_R3 complex exhibits a similar profile in this region of the difference spectrum (Figure 5), but of decreased magnitude implying fewer interactions of this type in 2(RF):O_R3.

(*C*) *Pyrimidine-Specific Interactions.* The presence of a methyl substituent at the pyrimidine C5 site is characterized by an intense Raman band at 1376 cm^{-1} that is sensitive to methyl group environment in nucleic acid secondary structures and methyl contacts in nucleoprotein complexes (Benevides et al., 1984, 1991a). Hydrophobic contacts involving the thymine exocyclic CH_3 group may be important determinants of repressor–operator recognition (Lewis et al., 1985; Takeda et al., 1989; Metzler & Lu, 1989). Since in the repressor–operator complexes the 1376-cm^{-1} band is not appreciably overlapped by protein bands, differences in the band profile can be assigned without ambiguity to changes in the environments of thymine methyl groups. Our data show that the 1376-cm^{-1} marker exhibits significantly increased intensity in each complex. We suggest that this increase is associated with shielding of thymine methyl groups by bound repressor, in accordance with the repressor–operator interface revealed in the co-crystal structure. As noted above for the guanine 6C=O interactions, the effect is greater for 2(RF):O_L1 than for 2(RF):O_R3

Discussion

Previous applications of laser Raman spectroscopy have defined conformationally sensitive vibrational features of nucleic acids, providing intrinsic probes for DNA and RNA structures in solution and crystal states (Benevides et al., 1984, 1986, 1988; Thomas & Wang, 1988). These studies facilitated the assignment of individual Raman bands to specific phosphodiester backbone geometries and nucleoside conformers (Table I). The resulting set of crystal-based structure markers is supported by normal coordinate calculations (Tsuboi et al., 1987) and has been exploited in structural analyses of oligonucleotides containing mismatched sequences (Benevides et al., 1989), RNA–DNA hybrid structures (Benevides & Thomas, 1988; Katahira et al., 1990), and viruses (Thomas, 1987; Thomas et al., 1988; Thomas & Serwer, 1990). Here we have sought to extend the general strategy by using the λ repressor–operator system to correlate Raman spectral features with protein–DNA interactions established from the solved co-crystal structures. Further, we have employed established correlations to identify and distinguish sites of molecular recognition in solution complexes of repressor with operators O_L1 and O_R3 and to compare the solution structures of the two λ operators. It is anticipated that the present results will aid development of an extended data base for the application of laser Raman spectroscopy to novel protein–DNA complexes, thus complementing X-ray and multidimensional NMR methods.

Previous Raman studies of protein–nucleic acid complexes have shown instances of significant perturbation to DNA secondary structure upon protein binding. Alteration of nucleoside sugar pucker, changes in the pattern of base stacking, and modification of the phosphate backbone geometry have been documented (Thomas et al., 1983, 1988; Incardona et al., 1987; Otto et al., 1987; Benevides et al., 1991a). In the case of filamentous bacteriophages, interaction of coat protein subunits with the packaged viral genome may be responsible for the unusual DNA structures stabilized in these viruses (Thomas et al., 1983, 1988). In addition to changes in DNA structure, changes in protein conformation may also accompany formation of complexes in solution. For example, a localized α-helix to β-sheet transition has been proposed in the DNA-binding of gp32 of bacteriophage T4 (Otto et al., 1987) and an α-helical folding transition has been shown to occur in the bZIP motif upon specific DNA binding (Weiss, 1990).

(*A*) *Raman Studies of the λ Repressor.* Raman spectroscopy of proteins provides information on both the peptide backbone conformation and selected side chain interactions (Spiro, 1987). Raman spectra are particularly informative of hydrogen-bonding interactions involving the phenolic OH group of tyrosine (Siamwiza et al., 1975). In an earlier Raman study of RF we determined the solution secondary structures of wild-type and genetically altered domains and deduced hydrogen-bonding states for individual tyrosines in both monomeric and dimeric forms of the protein (Thomas et al., 1986a). In this paper we have extended the earlier results to repressor–operator complexes. Importantly, Raman amide I and amide III secondary structure markers of RF are barely affected by complex formation, showing no significant alteration of protein secondary structure. Thus, unlike the bZIP domain, the HTH domain functions essentially as a preformed recognition element. In contrast to this invariance of HTH secondary structure, changes are observed in local side-chain environments.

The Raman intensity ratio I_{852}/I_{826}, which is diagnostic of the net hydrogen-bonding environment of repressor tyrosines, *decreases* from 2.05 in RF to 1.75 in 2(RF):O_L1, with an estimated experimental uncertainty of ±0.05 in each measured ratio (Thomas et al., 1986a). The present data alone do not identify the involved tyrosine(s). However, in the co-crystal structure, Y22 is positioned to allow its phenolic OH group to donate a hydrogen bond to the phosphate oxygen of the thymidylate residue T1 [designated "phosphate A1" in the notation of Jordan and Pabo (1988)]. Since, in the absence of DNA the phenolic OH group of Y22 functions exclusively as an acceptor (Thomas et al., 1986a), our data are consistent with the conversion of Y22 from the acceptor state (A) in the absence of DNA to the combined acceptor/donor state (E) in the 2(RF):O_L1 complex, in accordance with the proposed (Y22)O-H···O-P(T1) interaction in the co-crystal. Interestingly, Y22 is not part of the HTH motif. Its phenolic hydrogen bonding illustrates the presence of ancillary interactions in the complex. Mutation of Y22 to phenylalanine results in a more stable protein structure but reduces operator binding 15-fold (Hecht et al., 1985). Recent studies of families of mutant repressors generated by random cassette mutagenesis demonstrate that only tyrosine at this position is functional in vivo (Reidhaar-Olson & Sauer, 1990). In addition to tyrosine, aliphatic side chains of repressor exhibit Raman bands that are altered by complex formation, but the nature of the corresponding structure changes cannot be more specifically assessed.

For the 2(RF):O_R3 complex, we detect no change in the I_{852}/I_{826} ratio, which suggests that Y22 is not in position to make contact with the DNA in a fashion analogous to that found in the 2(RF):O_L1 complex. It is tempting to speculate that the path of the O_R3 helix axis differs from the bent

configuration observed in the O_L1 co-crystal structure (Jordan & Pabo, 1988), possibly a consequence of the polypurine–polypyrimidine sequence specific to the O_R3 nonconsensus domain.

(*B*) *Raman Studies of λ Operators.* The Raman phosphodiester and nucleoside conformation markers of both operators are those of right-handed B-DNA. Nevertheless, structural differences are observed between O_L1 and O_R3, presumably due to sequence-dependent variations involving the nonconsensus half-site. Such variations may serve as recognition signals for repressor binding and may contribute to the different affinities exhibited by λ repressor and Cro for cognate operator sites in the phage genome.

Interpretation of the spectra of O_L1 and O_R3 is based on previous studies of DNA fibers and crystals, which show that phosphodiester markers in the interval 800–840 cm^{-1} originate from gauche$^-$/trans/gauche$^+$ ($g^-/t/g^+$) conformations for $\alpha/\beta/\gamma$ torsions, whereas a marker near 850–860 cm^{-1} originates from an all-trans (t/t/t) conformation (Thomas et al., 1986b; Nishimura et al., 1986; Benevides et al., 1986, 1988, 1989). Accordingly, the shoulder present at 857 cm^{-1} in O_L1 but absent from O_R3 (which generates a weak trough in the Figure 6 difference spectrum) is consistent with a small percentage of O_L1 residues (10% or roughly 4 nucleotides) in the t/t/t conformation. The remaining 34 residues of O_L1, as well as all residues of O_R3, are deduced to be in the $g^-/t/g^+$ conformation. The difference spectrum of Figure 6 further suggests a net positive intensity for O_L1 near 826 cm^{-1} to compensate the net negative intensity at 857 cm^{-1}. A Raman marker near 826 cm^{-1} is characteristic of a $g^-/t/g^+$ domain containing GC pairs (Thomas et al., 1986b). Our results therefore suggest that a short domain comprising mainly GC pairs is configured differently in O_L1 (t/t/t) and O_R3 ($g^-/t/g^+$). Different backbone conformations in O_L1 and O_R3 are consistent with a large body of experimental evidence indicating that AT- and GC-rich domains of DNA exhibit slightly different phosphodiester geometries. This difference is presumably due to minor variations in torsion angles α and ζ associated with GC and AT pairs and may also reflect inequivalent phosphate–phosphate distances across the grooves of AT and GC tracts (Yoon et al., 1988).

The Raman marker near 855 cm^{-1} was analyzed in a study of the crystal structure of $[d(CCCCGGGG)]_2$ and assigned to the unusual phosphodiester conformation at the central CpG step (Benevides et al., 1986). In this structure the CpG step exhibits an all-trans (t/t/t) conformation, favorable to *interstrand* G-G base stacking (Haran et al., 1987). A similar conformation has also been described at the central TpA step in the crystal structure of $[d(CTCTAGAG)]_2$, which also accommodates interstrand purine–purine (A-A) stacking (Hunter et al., 1989). These findings suggest that analogous purine–purine stacking may account for the band at 857 cm^{-1} in O_L1. The sequences of the two operator sites (Figure 1) suggest two possible types of interstrand purine–purine stacking that may be present in O_L1 but absent from O_R3. The first would involve G8 in an interstrand run of five successive guanines (G12′-G11′-G8-G9′-G8′) including two CpG steps. The second would include A5′ in the run A11-G12-A5′-G14-G15. We attribute the observed 857-cm^{-1} band to either of these O_L1 segments. X-ray structures of $[d(CCCCGGGG)]_2$ and $[d(CTCTAGAG)]_2$ show that the t/t/t conformation imposes significantly different base stacking than the $g^-/t/g^+$ conformation (Haran et al., 1987; Hunter et al., 1989). The proposed t/t/t conformers of O_L1, absent from O_R3, could thus account for the remaining spectral differences of Figure 6, particularly the clusters of Raman difference bands in the 700–800- and 1200–1350-cm^{-1} intervals and the difference band near 1693 cm^{-1} (Small & Peticolas, 1971; Morikawa et al., 1973).

(*C*) *DNA Perturbations in Complexes.* The difference spectra of the repressor–operator complexes exhibit both positive and negative bands, most of which are relatively weak. This is in accordance with the co-crystal structure, which demonstrates that the interface involves a small number of protein and DNA functional groups (Anderson et al., 1987; Jordan & Pabo, 1988; Aggarwal et al., 1988; Mondragon et al., 1989; Pabo et al., 1990). The difference bands indicate perturbations to the DNA conformation as a consequence of repressor binding. Although complicated in origin, the bands indicate that AT base-pairs are more significantly altered by repressor binding than GC base-pairs in the O_L1 complex. In the co-crystal, the AT-rich ends of the repressor-bound operator differ from canonical B-DNA more significantly than the central GC-rich region (Jordan & Pabo, 1988).

The guanine ring generates an intense Raman band near 1490 cm^{-1} (Lord & Thomas, 1967; Small & Peticolas, 1971), which provides a marker for hydrogen-bond formation by 7N (Hartman et al., 1973; Nishimura et al., 1986). A shift in the band intensity identifies a minimum of two dG residues hydrogen bonded at 7N in the 2(RF):O_L1 complex. This may involve binding of the N-terminal arm to the central GC-rich region (Jordan & Pabo, 1988). For 2(RF):O_R3, the magnitude of the intensity shift is greatly reduced, which suggests fewer dG residues are hydrogen bonded at 7N. This may be the result of absent (or weakened) binding of the N-terminal arm with base-pair 8′ in the nonconsensus half-site. The contribution of the N-terminal arm to discrimination between operator sites has previously been proposed (Eliason et al., 1985).

Evidence for hydrogen bonding is also observed involving guanine 6C=O acceptors, as proposed for the interaction of G14′ and G12′ with O-H of S45 and N-H of K4, respectively (Jordan & Pabo, 1988). Hydrophobic contacts involving the thymine exocyclic CH_3 group are inferred from perturbations in the thymine-specific 1376-cm^{-1} band. These are likely to involve T1, T3, and T13′ of the consensus half-site and T1′ and T13 of the nonconsensus half-site. For O_R3, we note a reduction in the intensity of the difference band at 1376 cm^{-1}. This may result from the absence of a thymine at position 13 in the nonconsensus half-site of O_R3. Also, if the ends of the O_R3 helix are not bent to the same extent as those of O_L1, as visualized in the latter co-crystal structure, putative hydrophobic contacts involving T1 and T1′ with the γ carbon of Q44 and methylene carbons of E34 may not be realized for 2(RF):O_R3. The lack of a large intensity change at 840 cm^{-1} with repressor binding to O_R3 leads us to speculate that the AT-rich ends of the operator may not be as perturbed by repressor binding as those of the O_L1 complex.

Conclusions

Raman analysis of λ operators O_L1 and O_R3 in aqueous solution shows that both operator sites are members of the B-DNA genus but exhibit differences in the conformation of backbone phosphodiester bonds. These differences, which involve all-trans conformers of the torsions α, β, and γ at selected interstrand purine steps, presumably originate in their nonconsensus half-sites and may aid in the discrimination of related operator sites by the λ cI and Cro repressors. On complex formation, perturbations occur in Raman bands of both repressor and operator. Perturbations in the protein are minor and involve the conformations of side chains but not overall secondary structure. Although both operator sites

retain B-form secondary structure, the following significant changes are observed: (i) variations of nucleoside sugar pucker within the C2′-endo family; (ii) perturbation to phosphodiester group geometry at AT-rich domains; (iii) hydrogen-bond donation to guanine 7N sites exposed in the major groove; (iv) altered hydrogen bonding of guanine 6C=O acceptors; and (v) altered environments of thymine $5CH_3$ groups in the major groove. These perturbations are in accord with the crystal structure of the repressor–operator complex (Jordan & Pabo, 1988).

That the changes listed above are more pronounced for the 2(RF):O_L1 complex indicates that the number of contacts (base-specific hydrogen bonds, hydrophobic interactions of thymine methyl groups) between RF and O_R3 is significantly reduced. This reduction can be rationalized in terms of what is known about these contacts from the co-crystal structure (Jordan & Pabo, 1988) and the base sequence in the nonconsensus half-site of O_R3. Specifically, there is (i) an absence of terminal arm binding to base-pair 8′ due to the replacement of a GC by an AT base-pair at this position, (ii) a lack of a hydrophobic contact at position 13 due to the substitution of G for T, and (iii) a possible absence of T1 and T1′ interactions with protein hydrophobic groups as a consequence of a different helix geometry in the AT-rich ends of the repressor-bound O_R3 complex.

In this paper, we have shown that laser Raman spectroscopy offers prospects for determining specific interactions between proteins and nucleic acids in solution. In addition, protein–DNA interactions involving hydrogen bonding to guanine 7N and 6C=O acceptors have been demonstrated. Future studies will focus on comparative analyses of genetically altered repressors to identify the specific amino acids involved. The λ repressor–operator system provides a prototype for the further development of these methods.

Acknowledgments

M.A.W. thanks Profs. M. Karplus, D. J. Patel, and R. T. Sauer for support in the early stages of this work, C. O. Pabo for crystal coordinates and helpful discussion, A. Jeitler-Nillson and N. Fischbein for technical assistance, and F. Milanovich (Lawrence Livermore Laboratories) for encouragement. G.J.T. and J.M.B. thank Ms. Kelly Aubrey and Ms. Stacy Towse for assistance in sample preparation and Raman spectroscopy. Financial support from the National Institutes of Health is also gratefully acknowledged.

Registry No. Tyrosine, 60-18-4; guanine, 73-40-5; thymine, 65-71-4; adenine, 73-24-5; cytosine, 71-30-7.

References

Aggarwal, A. K., Rodgers, D. W., Drottar, M., Ptashne, M., & Harrison, S. C. (1988) *Science 242*, 899–907.

Anderson, J. E., Ptashne, M., & Harrison, S. C. (1987) *Nature 326*, 846–852.

Bellamy, L. J. (1980) *The Infrared Spectra of Complex Molecules, Vol. 2, Advances in Infrared Group Frequencies*, Chapman and Hall, New York.

Benevides, J. M., & Thomas, G. J., Jr. (1988) *Biochemistry 27*, 3868–3873.

Benevides, J. M., Wang, A. H.-J., van der Marel, G. A., van Boom, J. H., Rich, A., & Thomas, G. J., Jr. (1984) *Nucleic Acids Res. 12*, 5913–5925.

Benevides, J. M., Wang, A. H.-J., Rich, A., Kyogoku, Y., van der Marel, G. A., van Boom, J. H., & Thomas, G. J., Jr. (1986) *Biochemistry 25*, 41–50.

Benevides, J. M., Wang, A. H.-J., van der Marel, G. A., van Boom, J. H., & Thomas, G. J., Jr. (1988) *Biochemistry 27*, 931–938.

Benevides, J. M., Wang, A. H.-J., van der Marel, G. A., van Boom, J. H., & Thomas, G. J., Jr. (1989) *Biochemistry 28*, 304–310.

Benevides, J. M., Stow, P. L., Ilacz, L. L., Incardona, N. L., & Thomas, G. J., Jr. (1991a) *Biochemistry 30*, 4855–4863.

Benevides, J. M., Weiss, M. A., & Thomas, G. J., Jr. (1991b) *Biochemistry 30*, 4381–4388.

Dijkstra, S., Benevides, J. M., & Thomas, G. J., Jr. (1991) *J. Mol. Struct. 242*, 283–301.

Eliason, J. L., Weiss, M. A., & Ptashne, M. (1985) *Proc. Natl. Acad. Sci. U.S.A. 82*, 2339–2343.

Haran, T. E., Shakked, Z., Wang, A. H.-J., & Rich, A. (1987) *J. Biomol. Struct. Dyn. 5*, 199–217.

Hartman, K. A., Lord, R. C., & Thomas, G. J., Jr. (1973) in *Physicochemical Properties of Nucleic Acids* (Duchesne, J., Ed.) Vol. 2, pp 1–89, Academic Press, New York.

Hecht, M. H., Hehir, K. M., Nelson, H. C. M., Sturtevant, J. M., & Sauer, R. T. (1985) *J. Cell. Biochem. 29*, 217–224.

Hunter, W. N., D'Estaintot, B. L., & Kennard, O. (1989) *Biochemistry 28*, 2444–2451.

Incardona, N. L., Prescott, B., Sargent, D., Lamba, O. P., & Thomas, G. J., Jr. (1987) *Biochemistry 26*, 1532–1538.

Jordan, S. R., & Pabo, C. O. (1988) *Science 242*, 893–899.

Katahira, M., Lee, S. J., Kobayashi, Y., Sugeta, H., Kyogoku, Y., Iwai, S., Ohtsuka, E., Benevides, J. M., & Thomas, G. J., Jr. (1990) *J. Am. Chem. Soc. 112*, 4508–4512.

Lewis, M., Wang, J., & Pabo, C. (1985) in *Biological Macromolecules and Assemblies, Vol. 2, Nucleic Acids and Interactive Proteins* (Jurnak, F. A., & McPherson, A., Eds.) pp 265–287, Wiley, New York.

Lord, R. C., & Thomas, G. J., Jr. (1967) *Spectrochim. Acta 23A*, 2551–2591.

Metzler, W. J., & Lu, P. (1989) *J. Mol. Biol. 205*, 149–164.

Mondragon, A., Subbiah, S., Almo, S. C., Drottar, M., & Harrison, S. C. (1989) *J. Mol. Biol. 205*, 189–200.

Morikawa, K., Tsuboi, M., Takahashi, S., Kyogoku, Y., Mitsui, Y., Iitaka, Y., & Thomas, G. J., Jr. (1973) *Biopolymers 12*, 799–816.

Nishimura, Y., Tsuboi, M., Sato, T., & Akoi, K. (1986) *J. Mol. Struct. 146*, 123–153.

Otto, C., De Mul, F. F. M., & Greve, J. (1987) *Biopolymers 26*, 1667–1689.

Pabo, C. O., & Lewis, M. (1982) *Nature 298*, 443–447.

Pabo, C. O., Aggarwal, A. K., Jordan, S. R., Beamer, L. J., Obeysekare, U. R., & Harrison, S. C. (1990) *Science 247*, 1210–1213.

Prescott, B., Steinmetz, W., & Thomas, G. J., Jr. (1984) *Biopolymers 23*, 235–256.

Ptashne, M. (1986) *A Genetic Switch*, Cell Press, Cambridge, MA.

Reidhaar-Olson, J. F., & Sauer, R. T. (1990) *Proteins: Struct. Funct., Genet.* (in press).

Sauer, R. T., Hehir, K., Stearman, R. S., Weiss, M. A., Jeitler-Nilsson, A., Suchanek, E. G., & Pabo, C. O. (1986) *Biochemistry 25*, 5992–5998.

Siamwiza, M. N., Lord, R. C., Chen, M. C., Takamatsu, T., Harada, I., Matsuura, H., & Shimanouchi, T. (1975) *Biochemistry 14*, 4870–4876.

Small, E. W., & Peticolas, W. L. (1971) *Biopolymers 10*, 69–88.

Spiro, T. G., Ed. (1987) *Biological Applications of Raman Spectroscopy, Vol. 1, Raman Spectra and the Conforma-*

tions of Biological Macromolecules, Wiley Interscience, New York.
Takeda, Y., Sarai, A., & Rivera, V. M. (1989) *Proc. Natl. Acad. Sci. U.S.A. 86*, 439–443.
Thomas, G. J., Jr. (1970) *Biochim. Biophys. Acta 213*, 417–423.
Thomas, G. J., Jr. (1987) in *Biological Applications of Raman Spectroscopy, Vol. 1, Raman Spectra and the Conformations of Biological Macromolecules* (Spiro, T. G., Ed.) pp 135–201, Wiley Interscience, New York.
Thomas, G. J., Jr., & Wang, A. H.-J. (1988) in *Nucleic Acids and Molecular Biology* (Eckstein, F., & Lilley, D. M. J., Eds.) Vol. 2, pp 1–40, Springer-Verlag, Berlin.
Thomas, G. J., Jr., & Serwer, P. (1990) *J. Raman Spectrosc. 21*, 569–575.
Thomas, G. J., Jr., Prescott, B., & Day, L. A. (1983) *J. Mol. Biol. 165*, 321–356.
Thomas, G. J., Jr., Prescott, B., Benevides, J. M., & Weiss, M. A. (1986a) *Biochemistry 25*, 6768–6778.
Thomas, G. J., Jr., Benevides, J. M., & Prescott, B. (1986b) *Biomol. Stereodyn. 4*, 224–254.
Thomas, G. J., Jr., Prescott, B., Opella, S. J., & Day, L. A. (1988) *Biochemistry 27*, 4350–4357.
Tsuboi, M., Nishimura, Y., Hirakawa, A. Y., & Peticolas, W. L. (1987) in *Biological Applications of Raman Spectroscopy* (Spiro, T. G., Ed.) Vol. 2, pp 109–179, Wiley, New York.
Weiss, M. A. (1990) *Biochemistry 29*, 8020–8024.
Weiss, M. A., Pabo, C. O., Karplus, M., & Sauer, R. T. (1987) *Biochemistry 26*, 897–904.
Wolberger, C., Dong, Y., Ptashne, M., & Harrison, S. C. (1988) *Nature 316*, 789–795.
Yoon, C., Prive, G. G., Goodsell, D. S., & Dickerson, R. E. (1988) *Proc. Natl. Acad. Sci. U.S.A. 85*, 6332–6336.

Phosphorylation and Characterization of Bovine Heart Calmodulin-Dependent Phosphodiesterase†

Rajendra K. Sharma

Cell Regulation Group, Department of Medical Biochemistry, The University of Calgary, 3330 Hospital Drive N.W., Calgary, Alberta T2N 4N1, Canada

Received December 27, 1990; Revised Manuscript Received February 28, 1991

ABSTRACT: Calmodulin-dependent phosphodiesterase was purified to apparent homogeneity from the total calmodulin-binding fraction of bovine heart in a single step by immunoaffinity chromatography. The isolated enzyme had significantly higher affinity for calmodulin than the bovine brain 60-kDa phosphodiesterase isozyme. The cAMP-dependent protein kinase was found to catalyze the phosphorylation of the purified cardiac calmodulin-dependent phosphodiesterase with the incorporation of 1 mol of phosphate/mol of subunit. The phosphodiesterase phosphorylation rate was increased severalfold by histidine without affecting phosphate incorporation into the enzyme. Phosphorylation of phosphodiesterase lowered its affinity for calmodulin and Ca^{2+}. At constant saturating concentrations of calmodulin (650 nM), the phosphorylated calmodulin-dependent phosphodiesterase required a higher concentration of Ca^{2+} (20 μM) than the nonphosphorylated phosphodiesterase (0.8 μM) for 50% activity. Phosphorylation could be reversed by the calmodulin-dependent phosphatase (calcineurin), and dephosphorylation was accompanied by an increase in the affinity of phosphodiesterase for calmodulin.

Calmodulin-dependent cyclic nucleotide phosphodiesterase (3′,5′-cyclic-nucleotide 5′-nucleotidohydrolase, EC 3.1.4.17) is one of the key enzymes involved in the complex interactions between the cyclic nucleotide and Ca^{2+} second-messenger systems. Most tissues examined have been shown to contain calmodulin-dependent cyclic nucleotide phosphodiesterase activity [for reviews, see Beavo et al. (1982), Sharma et al. (1988), Beavo (1990), and Wang et al. (1990)]. The enzyme has been purified close to homogeneity from both bovine brain (Morrill et al., 1979; Sharma et al., 1980; Kincaid & Vaughan, 1983; Kincaid et al., 1984; Shenolikar et al., 1985) and bovine heart (LaPorte et al., 1979) and extensively characterized. Recent studies showed that calmodulin-dependent cyclic nucleotide phosphodiesterase exists in different isozymic forms (Hansen & Beavo, 1982; Sharma et al., 1984; Purvis et al., 1981; Vandermeers et al., 1983; Sharma & Wang, 1986a; Rossi et al., 1988) with different affinities for calmodulin (Mutus et al., 1985; Hansen & Beavo, 1986). Bovine brain calmodulin-dependent phosphodiesterase isozymes are differently regulated by phosphorylation (Sharma & Wang, 1985, 1986b,c). One of the isozyme forms, the 60-kDa subunit-containing isozyme from bovine brain, has been shown to be phosphorylated by adenosine cyclic 3′,5′-phosphate (cAMP)[1]-dependent protein kinase (Sharma & Wang, 1985, 1986b).

In this study, we examined the possible regulation of bovine heart calmodulin-dependent phosphodiesterase by cAMP-dependent protein kinase and observed that the rate of phosphorylation of this enzyme was significantly enhanced when histidine buffer was used in the phosphorylation reaction. Phosphorylation was accompanied by a decrease in affinity

† This work was supported by the Canadian Heart & Stroke Foundation and by Medical Research Council of Canada Grant MA-10672.

[1] Abbreviations: EGTA, ethylene glycol bis(β-aminoethyl ether)-*N,N,N′,N′*-tetraacetic acid; SDS, sodium dodecyl sulfate; EDTA, ethylenediaminetetraacetic acid; cAMP, adenosine cyclic 3′,5′-phosphate.

0006-2960/91/0430-5963$02.50/0